Ventilation strategies for front of neck airway rescue: an in silico study

Marianna Laviola[1#], Christian Niklas[1,2#], Anup Das[3], Declan G. Bates[3], Jonathan G. Hardman[1,4]

[1] Anaesthesia and Critical Care, Division of Clinical Neuroscience, School of Medicine, University of Nottingham, Nottingham NG7 2UH, UK

[2] Heidelberg University Hospital, Department of Anaesthesiology and Intensive Care, Im Neuenheimer Feld 110, 69120 Heidelberg, Germany

[3] School of Engineering, University of Warwick CV4 7AL, UK

[4] Nottingham University Hospitals NHS Trust, Nottingham NG7 2UH, UK

[#] These authors equally contributed to the paper.

Corresponding author

Dr Marianna Laviola

Anaesthesia & Critical Care, Division of Clinical Neuroscience

School of Medicine, University of Nottingham

Queen's Medical Centre, Nottingham NG7 2UH, UK

Tel +44 (0) 115 8231008

Email: marianna.laviola@nottingham.ac.uk

Abbreviated Title: Modelling front of neck ventilation

ABSTRACT

Background. During induction of general anaesthesia a "can't intubate, can't oxygenate" (CICO) situation can arise, leading to severe hypoxaemia. Evidence is scarce to guide ventilation strategies for small-bore front of neck airways that ensure effective oxygenation without risking lung damage and cardiovascular depression.

Methods. Fifty virtual subjects were configured using a high-fidelity computational model of the cardiovascular and pulmonary systems. Each subject breathed 100% oxygen for 3 minutes and then became apnoeic, with an obstructed upper airway. When arterial oxygen saturation reached 40%, front of neck airway access was simulated with various configurations. We examined the effect of several ventilation strategies on re-oxygenation, pulmonary pressures, cardiovascular function and oxygen delivery.

Results. Re-oxygenation was achieved in all ventilation strategies. Smaller airway configurations led to dynamic hyperinflation for a wide range of ventilation strategies. This effect was absent in the airways with larger internal diameter (≥3 mm). Intrapulmonary pressures rose quickly to supra-physiological values with the smallest airways, resulting in pronounced cardio-circulatory depression (cardiac output <3 L min^{-1} and mean arterial pressure <60 mmHg), impeding oxygen delivery (<600 ml min^{-1}). Limiting tidal volume (≤ 200 ml) and ventilatory frequency (≤ 8 breaths min^{-1}) for smaller diameter cannulas reduced dynamic hyperinflation and gas trapping, preventing cardiovascular depression.

Conclusions. Dynamic hyperinflation can be demonstrated for a wide range of front of neck cannulas when the upper airway is obstructed. When using small-bore cannulas in a CICO situation, ventilation strategies should be chosen that prevent gas trapping, to prevent severe adverse events, including cardio-circulatory depression.

Keywords: apnoea, airway management, airway obstruction, computational simulation, oxygenation.

INTRODUCTION

During a "can't intubate, can't oxygenate" (CICO) situation, the anaesthetist is unable to establish a patent airway through manipulation or conventional airway adjuncts and devices. In the patient who is rendered apnoeic, failure to manage the airway effectively for an extended period can result in severe hypoxaemia, progressing potentially to organ injury and death. In clinical practice, the occurrence of this scenario is rare, with approximately 1:12500 cases of general anaesthetics and 3–8:1000 tracheal intubation attempts in the emergency department.[1, 2]

Published guidance on airway management generally includes emergency tracheostomy / cricothyroidotomy as a rescue intervention.[2, 3] Despite evidence that the insertion of larger diameter airway devices is safer in these settings, the anatomical topography of insertion below the cricoid cartilage and the invasiveness and urgency of the procedure necessary to establish the airway often leads to the use of small diameter rescue airway cannulas and tubes. Small diameter airways produce high airflow resistances.[4] Due to incomplete exhalation, dynamic hyperinflation (commonly referred to as 'gas trapping' or 'stacking') can occur.[5, 6] This results in accumulation of intrathoracic gas volume, with increasing intrathoracic pressure, leading to cardiovascular depression and pulmonary injury. Due to known complications associated with over-distension and excessive ventilatory pressures, [1, 7] concerns have been raised regarding the safety of ventilation through small airway devices, when upper airway obstruction impedes the escape of excess gas from the lungs.[1, 8-14] Clinically, this scenario can occur where tumour, swelling or haematoma (or other causes of airway crowding) lead to obliteration of the periglottic airspace; the need for urgent front of neck access is more likely to arise in these settings.

Because CICO scenarios are rare, it is difficult to perform structured clinical research on optimal ventilation strategies for these situations. As a result, there is scarce evidence to provide specific guidance on how to achieve rapid re-oxygenation without risking lung damage and cardiovascular depression due to pulmonary over-distension.

In the past, animal studies,[15-17] mechanical lung models [4,18-20] and clinical data [13] have been employed to investigate the mechanics of ventilation via small airways and identify possible pitfalls in achieving safe oxygenation in this extreme situation. However, systematic clinical investigations to assess this scenario would be difficult to recruit and ethically challenging to perform. In addition, mechanical models are limited in their capacity to reproduce human physiology. Large animal models, present ethical limitations as well as intricate differences in their physiological setup, making it difficult to draw conclusions for extreme cases.

To address these challenges, high fidelity computer simulation of pathophysiological states and specific clinical interventions can be a powerful tool to inform future investigations or practice while circumventing the need to put patients at risk (or to use animal models for research).

The aim of this study is to evaluate various strategies for achieving re-oxygenation following airway rescue (i.e. re-opening the airway through a front of neck access with on-going upper airway obstruction) using a computer simulation of the integrated respiratory and cardiovascular systems. In particular, we investigated which combinations of tidal ventilation modalities assured safe intrapulmonary pressures when ventilating via narrow bore, front of neck airway devices.

METHODS

Computational model

This study uses the Interdisciplinary Collaboration in Systems Medicine (ICSM) simulation suite based upon the Nottingham Physiology Simulator.[21-24] The ICSM computer simulation is a highly-integrated, high fidelity computational model of a number of organ systems. The model has been extensively validated, including in the simulation of apnoea and hypoxaemia in adults.[25-27]

Recently, the ICSM simulation suite has been extended in order to include the physiological mechanisms underlying apnoeic oxygenation;[28] we previously used the updated model for an investigation of the influence of supraglottic oxygen supplementation on the effectiveness of airway rescue.[29]

A detailed description of the ICSM simulation suite is provided in the Supplemental Material.

Virtual subjects and protocol

A cohort of 50 in silico subjects was created, as per our previous work,[29] to represent the spectrum of physiology in an otherwise healthy population.

These subjects were developed by establishing credible physiological ranges for key model parameters based on data reported in the literature. The virtual subjects were generated using randomly permutated configurations of the parameters within these ranges (Table SM1).

For all virtual subjects, we simulated rescue ventilation with five different airway sizes (varying internal diameter [ID] and length based on real-world medical devices), as follows:

A. ID 1.8 mm, length 6.3 cm – representing the Ravussin 13G cannula (VBM Medical, GmbH, Sulz, Germany)
B. ID2.0 mm, length 7.5 cm – representing the Emergency Transtracheal Airway Catheter (Cook Medical)
C. ID 3.0 mm, length 5.8 cm – representing Patil's Airway [30]
D. ID 4.0 mm, length 6.3 cm – representing the Quicktrach cannula 4 mm ID (VBM Medical, GmbH, Sulz, Germany)
E. ID 6.0 mm, length 9.0 cm – representing the Melker cannula 6 mm ID (Cook, Bloomington, USA)

The 50 virtual subjects underwent pulmonary denitrogenation (pre-oxygenation) during resting, tidal breathing with an inspired oxygen fraction (F_IO_2) of 100% for 3 minutes. Induction of general anaesthesia was simulated, with apnoea and upper airway obstruction commencing simultaneously. Apnoea continued until the arterial oxygen saturation (SaO_2) reached 40%. At that time, the airway was opened (via front of neck access with each of the above device permutations) and various patterns of tidal ventilation with 100% oxygen were provided for 5 minutes.

The ventilation patterns comprised:

- Tidal volumes: 20, 50, 100, 200, 300, 400 and 500 ml
- Ventilatory frequencies: 4, 8, 12, 16 and 20 breaths min^{-1}
- Inspiratory to expiratory ratio (I:E): 1:2

The above patterns of tidal ventilation, in every combination, were repeated in all small-bore configurations considered (i.e. A, B and C). For the large-bore configurations (i.e. D and E) gas trapping was highly unlikely to occur according to previous investigations.[31] As our initial results indicated that gas trapping was indeed absent for all combinations of tidal volumes and ventilatory frequency in configuration D and E, the maximum tidal ventilation with a tidal volume of 500 ml and ventilatory frequency of 20 breaths min^{-1} was simulated as a control with the full bank of virtual subjects.

In a second step, we assessed safe intrapulmonary pressures for a wider range of airway size. To study the relationship between airway length and diameter, we ran a separate protocol with generic airway configurations (lengths 4–10 cm and internal diameters 1–4 mm). A grid of these configurations was assessed for resulting ventilator and airway pressures during ventilation with a tidal volume of 100 ml and ventilatory frequency of 8 breaths min^{-1}.

A total of 7,100 individual simulations were conducted to examine all the above scenarios.

Data collection

The following simulation outputs were recorded every 5 msec: end-inspiratory and end-expiratory lung pressures (calculated as the volume-weighted mean of alveolar compartmental pressures), ventilator pressure, lung volume, arterial haemoglobin oxygen saturation (SaO_2), arterial partial pressure of oxygen (PaO_2), arterial partial pressure of carbon dioxide ($PaCO_2$), arterial oxygen delivery (DO_2), cardiac output (CO), and mean arterial pressure (MAP). Data are presented as mean (standard deviation).

Model simulations were executed on a 64-bit Intel Core i7 3.7 GHz Windows 10 personal computer, running Matlab version R2018a.v9 (MathWorks Inc. MA, USA).

RESULTS

Figure 1 shows the mean values, calculated over the cohort of subjects, of end-inspiratory and end-expiratory lung pressures, and ventilator pressures for the small-bore configurations (i.e. A, B, C), during the application of the various patterns of tidal ventilation examined. When tidal volume was ≤200 ml and ventilator frequency was ≤8 breaths min^{-1}, the mean end-inspiratory lung pressure remained "safe" (i.e. less than 30 cmH_2O) in all airway configurations. In the smallest configuration (i.e. A) when tidal volume was 200 ml and ventilatory frequency was 8 breaths min^{-1}, although the ventilator pressure increased to 63.2 (0.7) cmH_2O, the end-inspiratory lung pressure was merely 21.8 (0.8) cmH_2O. For larger tidal volumes (i.e. 300 and 400 ml) only a ventilatory frequency of 4 breaths min^{-1} assured a mean end-inspiratory lung pressure <30 cmH_2O in all airway configurations. The largest tidal volume studied (500 ml) with a ventilatory frequency of 4 breaths min^{-1} resulted in a mean end-inspiratory lung pressure <30 cmH_2O in all airway configurations except in A.

The oxygenation goal following airway rescue, i.e. SaO_2 95%, was achieved in less than a minute for all patterns of ventilation studied, even when small tidal volumes and ventilatory frequencies were used (see Figure 2). In the smallest airway configurations (i.e. A and B), using larger tidal volumes ≥300 ml with ventilatory frequency 20 breaths min^{-1} caused re-oxygenation to be slower whereas in the airway configuration C, the time to reach SaO_2 95% was similar in all tidal ventilation patterns used.

In the large-bore configurations (D and E), despite a large minute ventilation (i.e. 500 ml x 20 breaths min^{-1}), no excessive intrapulmonary pressure was observed.

Example time courses of lung volume, PaO_2 and SaO_2 in one representative subject under varying ventilation strategies and airway sizes are illustrated in Figure 3. The different

experimental phases of pre-oxygenation, obstructed apnoea and ventilation via the rescue airway are demonstrated. Right and left panels show courses with the provision of the maximum (500 ml x 20 breaths min^{-1}) and minimum (20 ml x 4 breaths min^{-1}) patterns of the tidal ventilation, respectively. The middle panel shows the pattern of 200 ml x 8 breaths min^{-1} that still assured end-inspiratory pressure <30 cm H_2O in all airway configurations. When the maximum tidal ventilation pattern (i.e. 500 ml x 20 breaths min^{-1}) was applied, lung volumes showed a pronounced rise above FRC only in the smallest-bore airway configurations (i.e. A and B), indicating that for airway configurations with a diameter <3 mm, smaller tidal ventilation patterns should be used to avoid gas trapping and over-distension of the lung.

In all configurations, re-oxygenation was achieved even with the minimum pattern of tidal ventilation. Comparable time courses occurred in all modelled subjects.

Figure 4 shows the mean values, calculated over the cohort of the subjects, of end-inspiratory lung pressures (top panel), end-expiratory lung pressures (middle panel) and ventilator pressures (bottom panel) for a variation of airway lengths (4–10 cm) and diameters (1–4 mm) with a fixed minute ventilation (i.e. tidal volume 100 ml and ventilatory frequency 8 breaths min^{-1}). When airway diameter was 2 mm or more, end-inspiratory lung pressure remained less than 30 cm H_2O for all airway lengths.

Haemodynamic parameters, i.e. DO_2, CO and MAP, calculated during the 5 minutes of the tidal ventilation, for the small–bore airway configurations (i.e. A, B and C) are reported in Figure 5. DO_2 was more than 800 ml min^{-1} in configuration C for all patterns of tidal ventilation, whereas it dropped to 600 ml min^{-1} in configuration A and B as tidal volume and ventilatory frequency increased with a correspondent decrease in CO below 3 litres min^{-1} and in MAP below 60 mmHg. In particular, in configuration A, DO_2 dropped to 600 ml min^{-1} for tidal volume of 300 ml and ventilatory frequencies of 16 and 20 breaths min^{-1}, and for tidal volumes of 400 and 500 ml and ventilatory frequencies of 12, 16 and 20 breaths min^{-1}. In configuration B, DO_2 dropped for tidal volume of 300 ml and ventilatory frequency of 20 breaths min^{-1}, and for tidal volumes of 400 and 500 ml and ventilatory frequencies of 16 and 20 breaths min^{-1}.

In the large-bore configurations (i.e. D and E), DO_2, CO and MAP remained larger than 900 ml min^{-1}, 4.3 l min^{-1} and 85 mmHg, respectively, in all configurations.

As shown in Figure 6, although there was a significant rise in carbon dioxide when small tidal volumes were applied (i.e. ≤200 ml), oxygenation was assured in all airway configurations and for any pattern of ventilation considered at the end of the 5 minute rescue ventilation period.

DISCUSSION

In this computational modelling study, we simulated a CICO emergency scenario in a robust and representative cohort of 50 virtual subjects. In our investigation, both choosing larger airway diameters in front-of-neck access, or limiting minute ventilation for smaller diameter cannulas, reduced gas trapping. In vivo, dynamic hyperinflation leads to alveolar over-distension and consequent barotrauma, which are common complications of this rescue approach.[1, 2]

Our study provides new evidence that, in the case of front of neck airway rescue with an obstructed upper airway, larger airway configurations (internal diameter ≥3 mm) do not lead to increased airway pressures, gas trapping or excessive ventilation pressures (<30 cmH_2O).[32]

If the airway device's internal diameter is less than 3 mm, gas trapping becomes more pronounced as minute ventilation increases. In configurations A and B, ventilation caused excessive intrapulmonary pressures due to over-distension. This increase in lung volumes is demonstrated in Figure 3 as a result of dynamic hyperinflation in the context of the use of small bore cannulae, but not in the larger-gauge airway configurations. This behaviour reflects clinical experience, where reports from transtracheal jet ventilation note barotrauma as a known adverse event associated with front of neck access.[8-12] The gas trapping behaviour in the current study matches the findings of previous studies in mechanical lung models that investigated delayed expiration due to smaller diameters.[4] The increase in intrapulmonary pressure resulted in a decrease in mean arterial pressure, cardiac output and oxygen delivery (Figure 5). Particularly for the maximum minute ventilation scenarios in configurations A and B, severe cardiovascular depression was observed. This is in agreement with clinical experience where excessive intrapulmonary pressures can precipitate drastic cardio-circulatory compromise.

High ventilator pressures did not necessarily translate to high intrapulmonary pressures, e.g. in configuration A, using a tidal volume equal to 200 ml and a ventilatory frequency of 8 breaths min^{-1}, the ventilatory pressure was 63.2 (0.7) cm H_2O while end-inspiratory lung pressure was 21.8 (0.8) cm H_2O. Other authors frequently quote pre-systemic pressures in bar or psi. For consistency of units within the simulation we use cmH_2O. Ward and colleagues[33] showed that in a canine model a pre-systemic pressure translating to 3163 cmH_2O resulted in an airway pressure of only 22 cmH_2O with 80% upper airway obstruction. Biro and colleagues [34] made similar observations in a clinical study of 10 patients undergoing jet ventilation. In their case, driving pressures of 2099 and 3099 cmH_2O resulted in a peak

inspiratory pressure of 12.9 cmH_2O and 17.7 cmH_2O in complete upper airway obstruction, respectively. The significantly greater discrepancy between the driving pressure and the pressure delivered to the airway could easily be explained by different airflow dynamics. In the work of Biro,[34] the jet ventilation port of a rigid bronchoscope was used, the geometry of which was not specified. However, due to the tracheobronchial geometry of an adult patient, significantly longer tubing can be expected. In Ward's work,[33] a longer 13G cannula was used will have higher resistance. A linear relationship between cannula length and increased resistance can be inferred from Figure 4 in this study. Incomplete airway obstruction in Ward's study would also have allowed passive gas escape. This was shown by Sasano to prevent build-up of airway pressures on a mechanical lung model.[18]

Considering that safe oxygenation was possible via passive provision of high F_IO_2,[29] it is not surprising that even with minimal minute ventilation, safe oxygenation (SaO_2 95%) [35] was achieved in our present investigation. As CO_2 removal is efficiently achieved with higher minute ventilation (Figure 6) pursuing this goal would likely result in more pronounced gas trapping in smaller airway configurations. As re-oxygenation is the primary goal in an emergency front of neck access scenario, a volume-restricted ventilation strategy using F_IO_2 of 100% might be safer in small-bore cannulas, with tolerance of CO_2 accumulation.

The main limitation of our modelling approach is the inability to account for variations of airflow dynamics, like dislodgement of the cannula/device, misplacement into the surrounding soft tissue or dynamic fluctuations of airway resistances, such as bronchial secretions that could fully or partially occlude the small-bore devices. Similarly, we cannot simulate geometry of the airway devices as curvature or kinks might contribute significantly to airflow resistance.[36] Equally, the orientation of the airway device within the trachea cannot be simulated. It is difficult to gauge the effect these variations might have on the safety evaluation of the presented ventilation strategies. Furthermore, the simulated patients are assumed, to be free of cardiovascular morbidity – the effect of the more extreme intrathoracic pressures on pre-existing cardiac disease cannot be derived from our investigation. Also, the simulated complete upper airway obstruction is a specific scenario that might clinically not be as frequent as partial airway patency, allowing some escape of gas through a largely obstructed upper airway.

Unlike the previous work,[29] we used 50 virtual subjects instead of 100, because in this study the protocol considered a very large number of simulations, due to the massive number of permutations of rescue ventilation strategies. However, since the virtual subjects were generated using wide-ranging, random configurations of the key model parameters, 50 virtual subjects should be considered suitable and adequate to describe a wide spectrum of pathophysiology. Similarly, concessions were made in the simulated combinations of tidal

volume and ventilatory frequency to deal with limitations in computational power. The permutations presented cover a wide range of clinically feasible ventilation targets reaching moderately high minute ventilation, as well as volumes less than series dead-space volume. Simulations were conducted on a high-power desktop PC; upscaling of computational resource to high performance computing would allow for wider coverage of potential treatment and subject permutations.

For future studies, it would be interesting to investigate more extensive variations in I:E ratio. Additionally, adaptation of the model allowing active inhalation and exhalation [15-17, 37] could inform the discussion about devices that facilitate this type of ventilation, potentially reducing gas trapping. Finally, it will be useful to study partial (and absent) upper airway obstruction while simulating small-bore airway ventilation – in particular, the dynamic venting of pressure from the lungs against an increased airway resistance from partial obstruction. Simulation of incomplete upper airway obstruction will most likely affect the tendency for gas trapping, the efficiency of ventilation/oxygenation and of CO_2 removal, as suggested by previous studies.[38]

AUTHOR'S CONTRIBUTIONS

Design of study: ML, CN, AD, JGH

Simulation runs: ML

Interpretation of data: ML, CN, AD, DGB, JGH

Writing and final approval of manuscript: ML, CN, AD, DGB, JGH

ACKNOWLEDGMENTS

The authors acknowledge the following funding that contributed to the conduct of this investigation:

- EPSRC grant "Personalised simulation technologies for optimising treatment in the intensive care unit: realising industrial and medical applications" (EP/P023444/1)
- Fisher and Paykel Healthcare (New Zealand): sponsorship of research into apnoea and mechanisms of gas exchange.

DECLARATION OF INTERESTS

JGH is Associate Editor-in-Chief of the British Journal of Anaesthesia. JGH accepts fees for the provision of advice to the police, crown prosecution service, coroners and solicitors.

The other authors have no conflicts to declare.

FUNDING STATEMENT

UK Engineering and Physical Sciences Research Council (grants EP/P023444/1).

Fisher and Paykel Healthcare (New Zealand): sponsorship of research into apnoea and mechanisms of gas exchange.

SUPPLEMENTARY MATERIAL

Supplementary material is available online.

REFERENCES

1 Duggan LV, Ballantyne Scott B, Law JA, Morris IR, Murphy MF, Griesdale DE. Transtracheal jet ventilation in the 'can't intubate can't oxygenate' emergency: a systematic review. *Br J Anaesth* 2016; **117 Suppl 1**: i28-i38
2 Cook TM, Woodall N, Frerk C. Major complications of airway management in the UK: results of the Fourth National Audit Project of the Royal College of Anaesthetists and the Difficult Airway Society. Part 1: Anaesthesia†. *Br J Anaesth* 2011; **106**: 617-31
3 Frerk C, Mitchell VS, McNarry AF, et al. Difficult Airway Society 2015 guidelines for management of unanticipated difficult intubation in adults. *Br J Anaesth* 2015; **115**: 827-48
4 Dworkin R, Benumof JL, Benumof R, Karagianes TG. The effective tracheal diameter that causes air trapping during jet ventilation. *J Cardiothorac Anesth* 1990; **4**: 731-6
5 Blanch L, Bernabé F, Lucangelo U. Measurement of Air Trapping, Intrinsic Positive End-Expiratory Pressure, and Dynamic Hyperinflation in Mechanically Ventilated Patients. *Respiratory Care* 2005; **50**: 110-24
6 Gemma M, Nicelli E, Corti D, et al. Intrinsic positive end-expiratory pressure during ventilation through small endotracheal tubes during general anesthesia: incidence, mechanism, and predictive factors. *Journal of clinical anesthesia* 2016; **31**: 124-30
7 Tuxen DV, Lane S. The effects of ventilatory pattern on hyperinflation, airway pressures, and circulation in mechanical ventilation of patients with severe air-flow obstruction. *Am Rev Respir Dis* 1987; **136**: 872-9
8 Benumof JL, Scheller MS. The Importance of Transtracheal Jet Ventilation in the Management of the Difficult Airway. *Anesthesiology* 1989; **71**: 769-78
9 Monnier PH, Rauvissin P, Savary M, Freeman J. Percutaneous transtracheal ventilation for laser endoscopic treatment of laryngeal and subglottic lesions. *Clin Otolaryngol Allied Sci* 1988; **13**: 209-17
10 Jacobs HB, Smyth NPD, Witorsch P. Transtracheal Catheter Ventilation: Clinical Experience in 36 Patients. *Chest* 1974; **65**: 36-40
11 Chandradeva K, Palin C, Ghosh SM, Pinches SC. Percutaneous transtracheal jet ventilation as a guide to tracheal intubation in severe upper airway obstruction from supraglottic oedema. *Br J Anaesth* 2005; **94**: 683-6
12 Craft TM, Chambers PH, Ward ME, Goat VA. Two cases of barotrauma associated with transtracheal jet ventilation. *Br J Anaesth* 1990; **64**: 524-7
13 Bourgain JL, Desruennes E, Cosset MF, Mamelle G, Belaiche S, Truffa-Bachi J. Measurement of end-expiratory pressure during transtracheal high frequency jet ventilation for laryngoscopy. *Br J Anaesth* 1990; **65**: 737-43
14 Cook TM, Bigwood B, Cranshaw J. A complication of transtracheal jet ventilation and use of the Aintree intubation catheter® during airway resuscitation. *Anaesthesia* 2006; **61**: 692-7
15 de Wolf MWP, Gottschall R, Preussler NP, Paxian M, Enk D. Emergency ventilation with the Ventrain® through an airway exchange catheter in a porcine model of complete upper airway obstruction. *Can J Anaesth* 2017; **64**: 37-44
16 Hamaekers AEW, Götz T, Borg PAJ, Enk D. Achieving an adequate minute volume through a 2 mm transtracheal catheter in simulated upper airway obstruction using a modified industrial ejector. *Br J Anaesth* 2010; **104**: 382-6
17 Hamaekers AE, van der Beek T, Theunissen M, Enk D. Rescue ventilation through a small-bore transtracheal cannula in severe hypoxic pigs using expiratory ventilation assistance. *Anesth Analg* 2015; **120**: 890

18 Sasano N, Tanaka A, Muramatsu A, et al. Tidal volume and airway pressure under percutaneous transtracheal ventilation without a jet ventilator: comparison of high-flow oxygen ventilation and manual ventilation in complete and incomplete upper airway obstruction models. *J Anesth* 2014; **28**: 341-6
19 Meissner K, Iber T, Roesner J-P, et al. Successful Transtracheal Lung Ventilation Using a Manual Respiration Valve: An In Vitroand In VivoStudy. *Anesthesiology* 2008; **109**: 251-9
20 Flint NJ, Russell WC, Thompson JP. Comparison of different methods of ventilation via cannula cricothyroidotomy in a trachea–lung model. *Br J Anaesth* 2009; **103**: 891-5
21 Hardman JG, Bedforth NM, Ahmed AB, Mahajan RP, Aitkenhead AR. A physiology simulator: validation of its respiratory components and its ability to predict the patient's response to changes in mechanical ventilation. *Br J Anaesth* 1998; **81**: 327-32
22 Hardman JG, Bedforth NM. Estimating venous admixture using a physiological simulator. *Br J Anaesth* 1999; **82**: 346-9
23 Bedforth NM, Hardman JG. Predicting patients' responses to changes in mechanical ventilation: a comparison between physicians and a physiological simulator. *Intensive Care Med* 1999; **25**: 839-42
24 Das A, Gao Z, Menon PP, Hardman JG, Bates DG. A systems engineering approach to validation of a pulmonary physiology simulator for clinical applications. *J R Soc Interface* 2011; **8**: 44-55
25 McNamara MJ, Hardman JG. Hypoxaemia during open-airway apnoea: a computational modelling analysis. *Anaesthesia* 2005; **60**: 741-6
26 McClelland SH, Bogod DG, Hardman JG. Pre-oxygenation and apnoea in pregnancy: changes during labour and with obstetric morbidity in a computational simulation. *Anaesthesia* 2009; **64**: 371-7
27 Pillai A, Chikhani M, Hardman JG. Apnoeic oxygenation in pregnancy: a modelling investigation. *Anaesthesia* 2016; **71**: 1077-80
28 Laviola M, Das A, Chikhani M, Bates DG, Hardman JG. Computer simulation clarifies mechanisms of carbon dioxide clearance during apnoea. *Br J Anaesth* 2019; **122**: 395-401
29 Laviola M, Niklas C, Das A, Bates DG, Hardman JG. Effect of oxygen fraction on airway rescue: a computational modelling study. *Br J Anaesth* 2020; **125**: 69-74
30 Vadodaria BS, Gandhi SD, McIndoe AK. Comparison of four different emergency airway access equipment sets on a human patient simulator*. *Anaesthesia* 2004; **59**: 73-9
31 Craven RM, Vanner RG. Ventilation of a model lung using various cricothyrotomy devices*. *Anaesthesia* 2004; **59**: 595-9
32 Ventilation with Lower Tidal Volumes as Compared with Traditional Tidal Volumes for Acute Lung Injury and the Acute Respiratory Distress Syndrome. *New England Journal of Medicine* 2000; **342**: 1301-8
33 Ward KR, Menegazzi JJ, Yealy DM, Klain MM, Molner RL, Goode JS. Translaryngeal jet ventilation and end-tidal PCO2 monitoring during varying degrees of upper airway obstruction. *Ann Emerg Med* 1991; **20**: 1193-7
34 Biro P, Layer M, Becker HD, et al. Influence of airway-occluding instruments on airway pressure during jet ventilation for rigid bronchoscopy. *Br J Anaesth* 2000; **85**: 462-5
35 Beachey W. Clinical Assessment of Acid-Base and Oxygenation Status. *Respiratory Care Anatomy and Physiology Foundations for Clinical Practise*: Elsevier, 2012
36 Manczur T, Greenough A, Nicholson GP, Rafferty GF. Resistance of pediatric and neonatal endotracheal tubes: influence of flow rate, size, and shape. *Crit Care Med* 2000; **28**: 1595-8
37 Hamaekers A, Borg P, Enk D. The importance of flow and pressure release in emergency jet ventilation devices. *Paediatr Anaesth* 2009; **19**: 452-7

38 de Wolf M, van der Beek T, Hamaekers A, Theunissen M, Enk D. A prototype small-bore ventilation catheter with a cuff: cuff inflation optimizes ventilation with the Ventrain. *Acta Anaesthesiol Scand* 2018; **62**: 328-35
39 Network TARDS. Ventilation with Lower Tidal Volumes as Compared with Traditional Tidal Volumes for Acute Lung Injury and the Acute Respiratory Distress Syndrome. *New England Journal of Medicine* 2000; **342**: 1301-8
40 Amato MB, Meade MO, Slutsky AS, et al. Driving pressure and survival in the acute respiratory distress syndrome. *N Engl J Med* 2015; **372**: 747-55

FIGURE LEGENDS

Figure 1. Mean values, calculated over the cohort of 50 in silico subjects, of end-expiratory lung pressure, end-inspiratory lung pressure and ventilator pressure (bottom panels) for airway configurations A (inner diameter 1.8 mm, length 6.3 cm), B (inner diameter 2.0 mm, length 7.5 cm) and C (inner diameter 3.0 mm, length 5.8 cm). Standard deviations have not been reported for graphical reasons and because they were not significant. Levels of pressures were represented with different colour coding; green represented "safe" pressures (<30 cm H_2O),[39] yellow represented pressures 30–60 cm H_2O, and red represented high pressures (>60 cm H_2O). These thresholds have been chosen due to clinical consideration and indicative studies showing a proportional relationship between driving pressures and potential patient harm in other patient cohorts[40] where a plateau pressure level greater than 30 cm H_2O might be acceptable under certain conditions.

Figure 2. Time taken to achieve arterial haemoglobin oxygen saturation (SaO_2) of 95% in the small-bore airway configuration (i.e. A, B, and C) during all patterns of tidal ventilation studied. Vf ventilatory frequency (breaths min^{-1}); Vt tidal volume (ml).

Figure 3. Time-course of lung volumes, PaO_2 and SaO_2, during pre-oxygenation, apnoea, and airway opening with different provisions of tidal ventilation in a representative subject; right panel: tidal volume 20 ml and ventilatory frequency 4 breaths $min^{-1;}$ middle panel: tidal volume 200 ml and ventilatory frequency 8 breaths min^{-1}; left panel: tidal volume 500 ml and ventilatory frequency 20 breaths min^{-1}.

Figure 4. End-inspiratory lung pressure, end-expiratory lung pressure and ventilator pressure for various airway lengths and diameters, with tidal volume 100 ml and ventilatory frequency 8 breaths min^{-1}. Green areas: pressure <30 cm H_2O; yellow areas pressures 30–60 cm H_2O and red areas: pressures >60 cm H_2O.

Figure 5. Arterial oxygen delivery (DO_2), cardiac output (CO), and mean arterial pressure (MAP) in the small-bore configurations (i.e. A, B and C) at the end of tidal ventilation provision. Before the opening of the obstructed airway (i.e. at the end of apnoea), DO_2, CO and MAP were 227.2 (22.9) ml min^{-1}, 2.7 (0.1) l $min^{-1}$and 57.2 (2.7) mmHg, respectively. Vf ventilatory frequency (breaths min^{-1}); Vt tidal volume (ml).

Figure 6. Arterial partial pressure of oxygen (PaO_2) and carbon dioxide ($PaCO_2$), calculated in the small-bore configurations (i.e. A, B and C) at the end of tidal ventilation provision. Before the opening of the obstructed airway (i.e. at end of apnoea), PaO_2 and $PaCO_2$ were 3.8 (0.1) kPa and 11.1 (1) kPa, respectively. Vf ventilatory frequency (breaths min^{-1}); Vt tidal volume (ml).

Figure 1

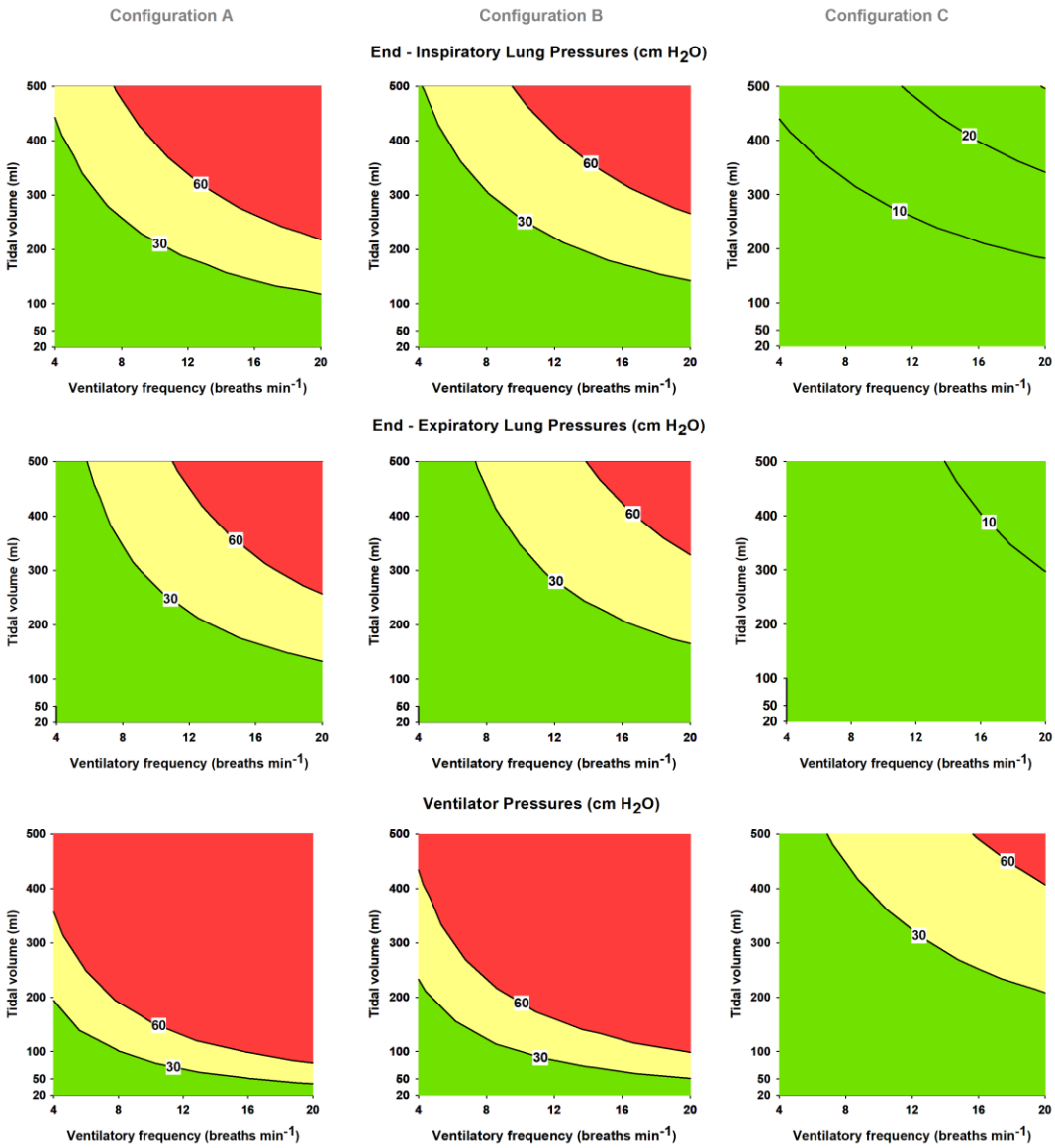
Configuration A
Configuration B
Configuration C
End - Inspiratory Lung Pressures (cm H2O)
End - Expiratory Lung Pressures (cm H2O)
Ventilator Pressures (cm H2O)
Tidal volume (ml)
Ventilatory frequency (breaths min-1)
500
400
300
200
100
50
20
4
8
12
16
20
60
30
20
10

Figure 2

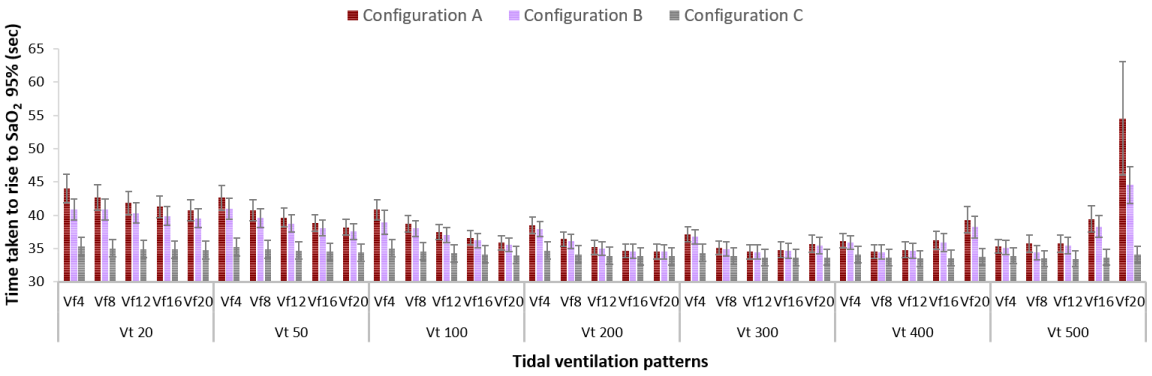
Configuration A
Configuration B
Configuration C
Time taken to rise to SaO2 95% (sec)
65
60
55
50
45
40
35
30
Vf4 Vf8 Vf12 Vf16 Vf20
Vt 20
Vt 50
Vt 100
Vt 200
Vt 300
Vt 400
Vt 500
Tidal ventilation patterns

Figure 3

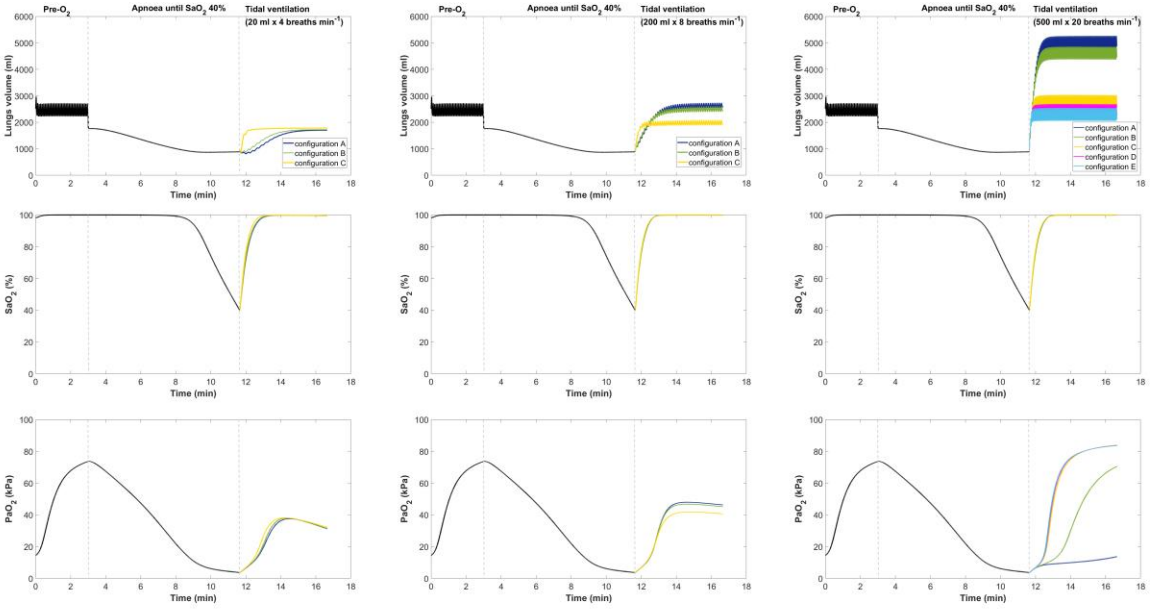
Pre-O2
Apnoea until SaO2 40%
Tidal ventilation
(20 ml x 4 breaths min-1)
(200 ml x 8 breaths min-1)
(500 ml x 20 breaths min-1)
Lungs volume (ml)
SaO2 (%)
PaO2 (kPa)
Time (min)
configuration A
configuration B
configuration C
configuration D
configuration E

Figure 4

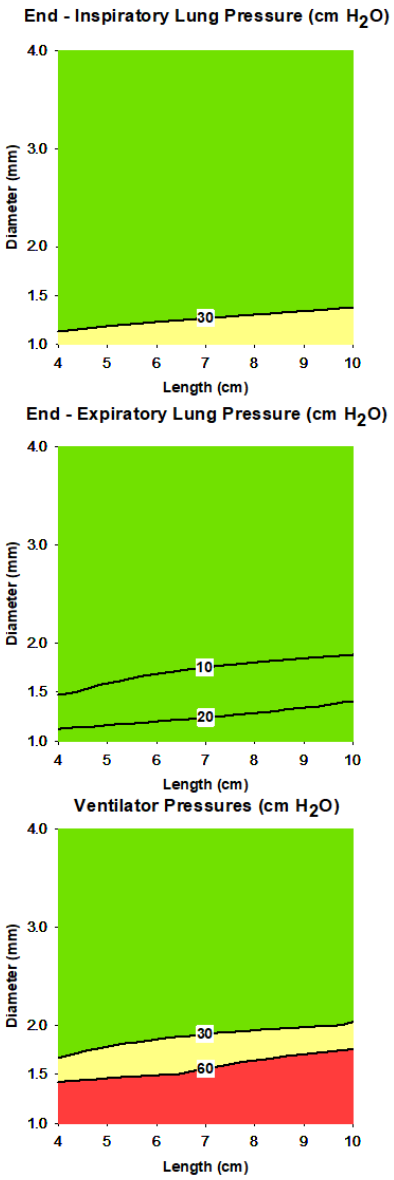
End - Inspiratory Lung Pressure (cm H_2O)
Diameter (mm)
4.0
3.0
2.0
1.5
1.0
30
4
5
6
7
8
9
10
Length (cm)
End - Expiratory Lung Pressure (cm H_2O)
Diameter (mm)
4.0
3.0
2.0
1.5
1.0
10
20
4
5
6
7
8
9
10
Length (cm)
Ventilator Pressures (cm H_2O)
Diameter (mm)
4.0
3.0
2.0
1.5
1.0
30
60
4
5
6
7
8
9
10
Length (cm)

Figure 5

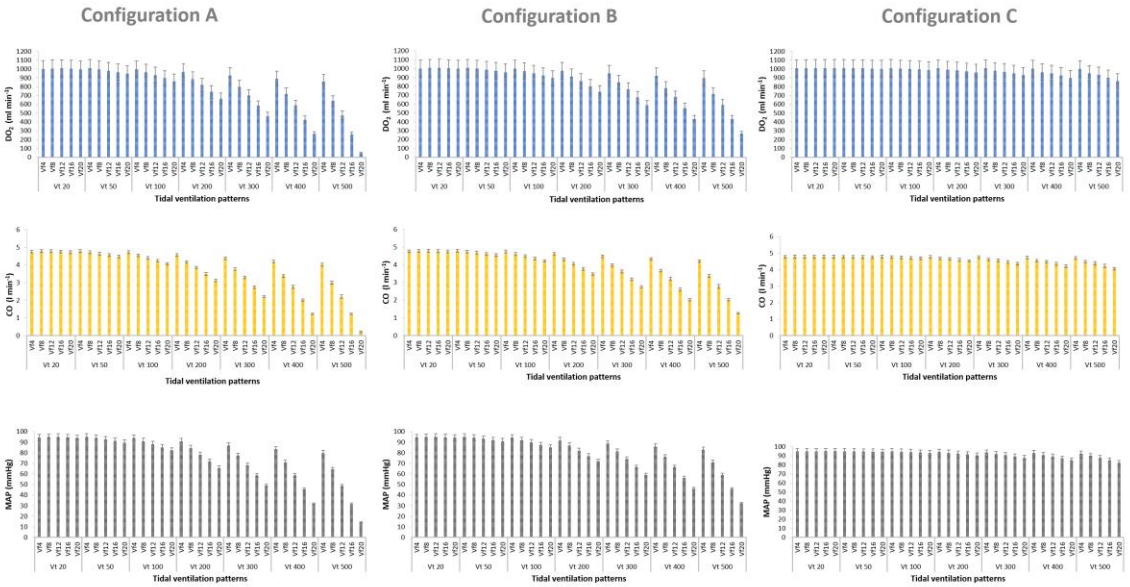
Configuration A
Configuration B
Configuration C
DO2 (ml min-1)
CO (l min-1)
MAP (mmHg)
Tidal ventilation patterns
Vt 20
Vt 50
Vt 100
Vt 200
Vt 300
Vt 400
Vt 500

Figure 6

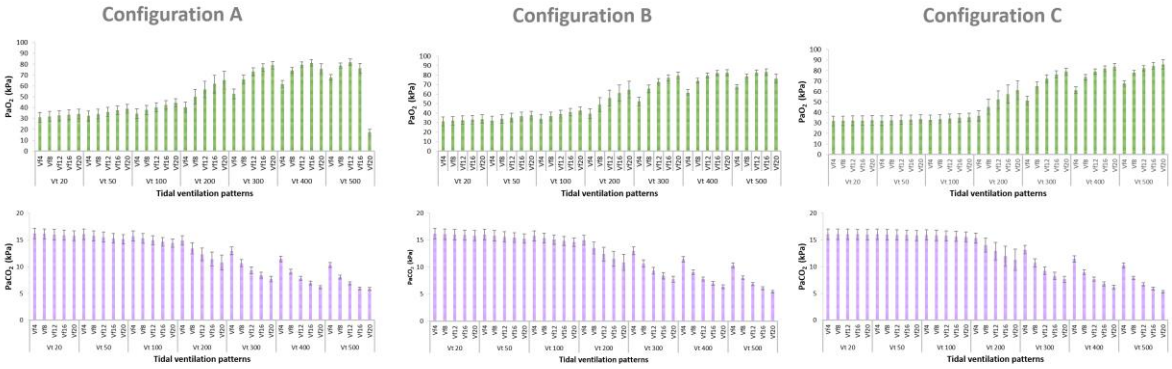
Configuration A
Configuration B
Configuration C
PaCO2 (kPa)
Tidal ventilation patterns
Vt 20
Vt 50
Vt 100
Vt 200
Vt 300
Vt 400
Vt 500